Once the working region was fixed, mechanical optimization of the structure was done so as to have a 1µm/g of mechanical sensitivity in the *y*-axis under *y* acceleration. Considering the slope of the linear regions of the fig. 4.38b, it can be seen that the designed accelerometer is expected to have an optical sensitivity of >4dB/g.

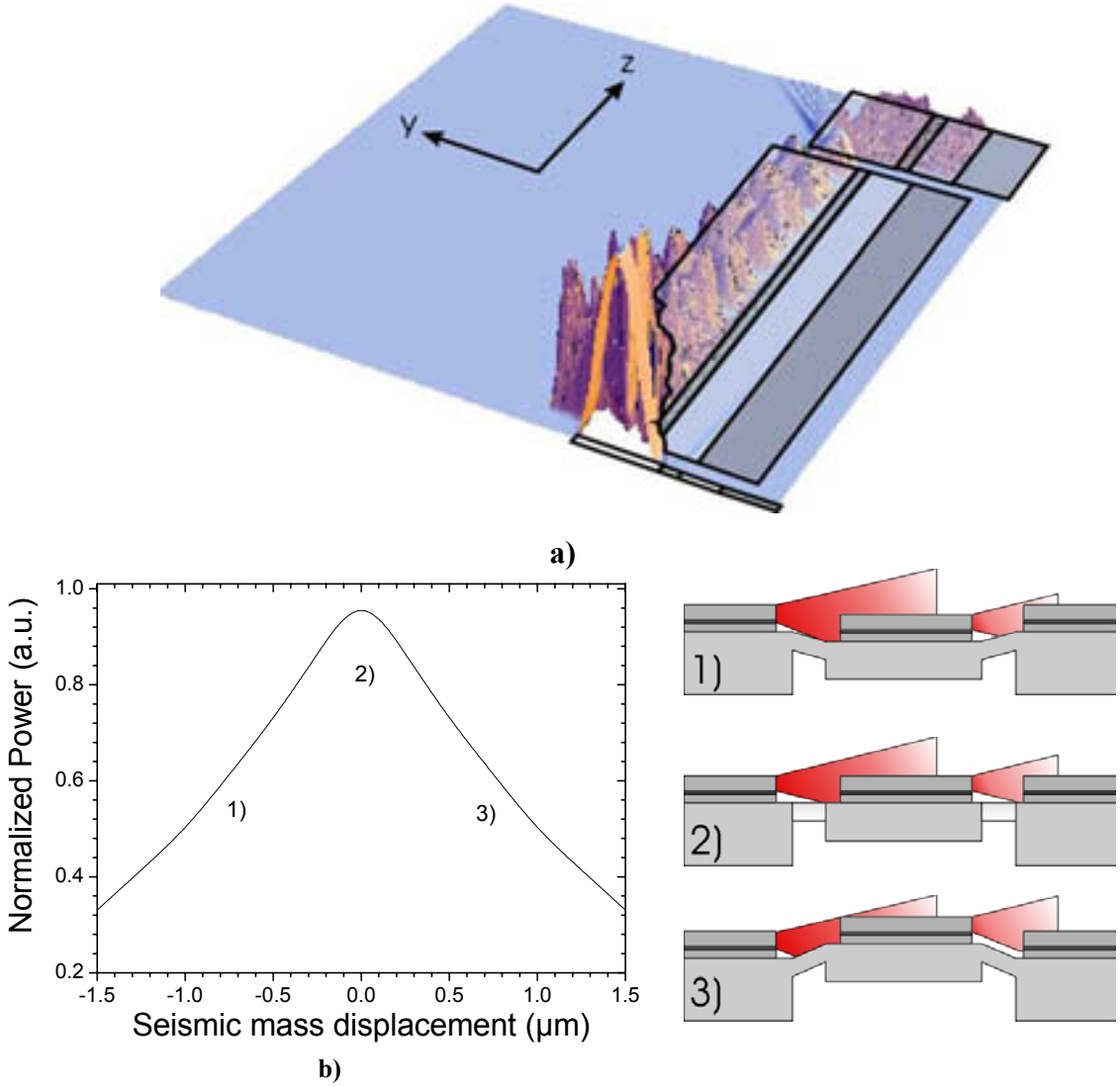

Fig 4.38. a) Normalized intensity propagation in an 50% misalignment between the input/output and the sensing waveguide. b) Normalized power as a function of the seismic mass displacement.

The most significant difference in the mechanical configuration as compared to the diaphragm accelerometers is due to the sensitivity in the *y*-axis for which the misalignment accelerometers have been designed. Clearly, the structure should have a lower stiffness if measurements of a magnitude 50 times smaller were to be done. For a given mass, more sensitive devices can be obtained by enlarging the bridges, either

orthogonal or parallel to the seismic mass edge. Although the latter has proved to have higher sensitivity, it is larger in size, which means more silicon consumption and more expensive devices. Thence, parallel bridges have been selected for misalignment-based optical accelerometers.

When a *y* acceleration of 1g was applied on the device, the movement in the *y*-axis is shown in fig. 4.39a. An expectable flat movement of the mass is observed. Crossed accelerations when 1g acceleration was applied to the *y*-axis (fig. 4.39b) and to the *x* axis (4.39c) have also been obtained. However, due to the device design, it can be observed that the symmetry plane along *y* remains unperturbed when there are *z*-accelerations, being the device completely insensitive to these speed variations.

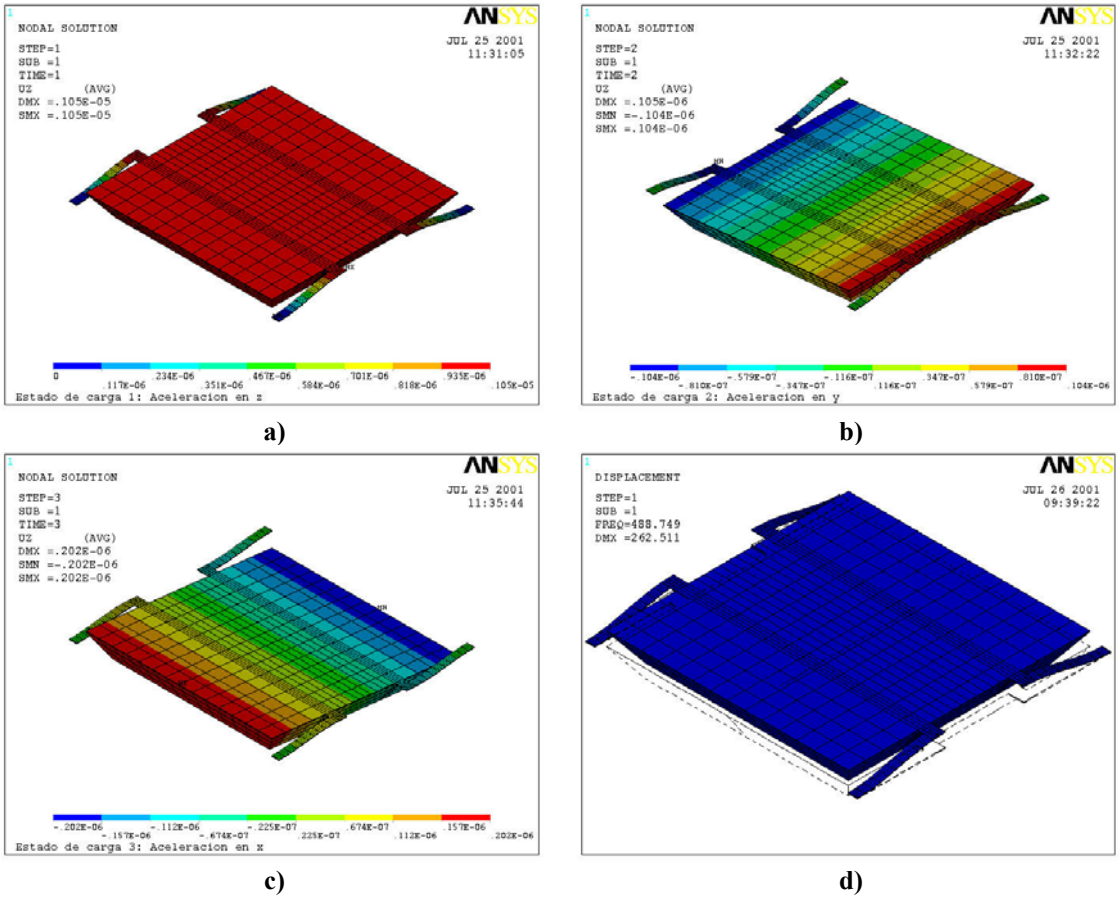

Fig 4.39. Displacement of the misalignment accelerometer in the *y*-axis for an acceleration in the *y* axis a), in the *z* axis b) and in the *x* axis c). First vibrational mode is presented in d).